

AguaClara Cornell Floc Modeling

Fall 2025: Final Report

Alex Gardocki (rag325), Lauren Hsu (lkh58), Sarvesh Prabhu (sp2572), Aaron Gu (ag2698), Irene Ma (im398), Aronya Sarker (as4447)

December 8, 2025

Abstract

The Floc Modeling subteam aims to further our understanding of the mechanics of floc formation and clarification in order to improve performance in AguaClara plants through the development of a mathematical model of these processes. This semester, our team is focusing on evaluating the distribution of flocs within the clarifier to test the assumptions of the floc filter clarification model. To analyze the distribution of flocs experimentally, we are employing dye tracers to track the formation and movement of flocs within the floc filter. This will provide evidence to support or refute the assumption that floc saturation is distributed uniformly throughout the floc filter. By combining these experimental results with ongoing efforts to verify our existing models via simulation, we can gain further confidence in our understanding of the mechanisms underlying flocculation and clarification.

Introduction

Flocculation and clarification are critical to the AguaClara treatment process as they remove most primary particles before filtration and chlorination. While these processes are widely used throughout the water treatment industry, gaps remain in our understanding of their underlying physical mechanisms. This lack of understanding has made it challenging to optimize the design of treatment plants and develop automated systems that can successfully respond to fluctuating conditions. It has also prevented the widespread adoption of the novel floc filter technology used in AguaClara plants during clarification. For these reasons, an accurate mathematical model of these processes is essential.

This semester, the Floc Modeling subteam is focusing its efforts on refining the AguaClara clarification model. Clarification is the process following flocculation in which flocs are separated from treated water through settling, also known as sedimentation. During conventional clarification, sedimentation is the sole mechanism for particle removal. However, AguaClara plants utilize an additional process called floc sweeping. Floc sweeping allows previously formed flocs to capture additional primary particles that would settle too slowly on their own, increasing the overall efficiency of clarification. In order to achieve this, vertical jets of water are used to maintain a suspension of flocs known as the floc filter. Primary particles travel up through this suspension, colliding and aggregating with the suspended flocs, which can then be removed. Smaller flocs travel up towards a set of plate settlers, which aggregate these small flocs into larger ones that eventually settle back into the floc filter.

Floc sweeping efficiency depends on coagulant dose, floc filter concentration, and floc saturation. Flocs are initially very porous; as a floc captures primary particles, its pores fill. Eventually, a floc cannot capture any additional particles. Floc saturation is a measurement characterizing how “full” a floc is and how many more particles it is able to capture. Spatial variations in floc saturation within the clarifier can affect particle removal efficiency in the clarifier. If a mathematical model can predict the spatial distribution of flocs in the clarifier, then the areas of the clarifier with the most saturated flocs can be targeted first during wasting. Thus, only flocs that are still capable of capturing primary particles will remain in the clarifier, increasing clarification efficiency.

This semester, the Floc Modeling subteam is investigating the physical properties and interactions between flocs and primary particles in the floc filter during clarification through the use of a lab-scale model vertical clarifier. This model clarifier allows for observation of the floc filter in order to monitor spatial variations in floc filter concentration and floc saturation as well as effluent turbidity under different coagulant dosages and influent conditions. The compact size of the clarifier leads to a low hydraulic residence time, allowing for rapid experimentation and iteration.

Building off the work of the Summer 2025 team, the current subteam is exploring an alternative experimental approach. Rather than tracking floc saturation directly, it relies upon tracking the movement of tracer flocs within the floc filter. This will allow the team to analyze the distribution of flocs within the floc filter and to determine whether or not the floc filter is well-mixed. The results of these experiments can then be applied to validate the assumption of uniform floc saturation within the floc filter.

Previous Work

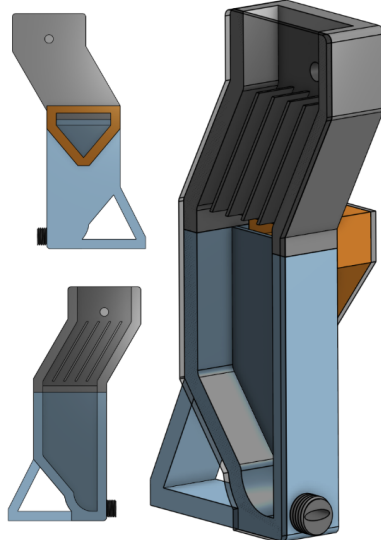


Figure 1. Schematic of prototype model clarifier.

The Spring 2025 team developed the clarifier shown in Figure 1, and it successfully demonstrated the ability to form a floc filter.

Unfortunately, the grey resin back of the Spring 2025 clarifier made it difficult to distinguish color variations within the clarifier. This was particularly problematic when attempting to analyze the distribution of floc saturation within the floc filter as the proposed method for measuring floc saturation relied upon using colored primary particles to incite a color difference in more saturated regions. The opaque back also prevented the floc filter from being backlit. According to Hurst et al. (2014b), backlighting the floc filter would allow the spatial distribution of floc concentration to be measured via image capture.

For these reasons, the Summer 2025 team redesigned and fabricated a new clarifier, shown in Figure 2, to improve upon the Spring 2025 version. Major changes included utilizing an acrylic plate for both the front and back of the clarifier and adding sampling ports at different heights within the floc filter for taking samples or targeting the removal of saturated flocs. Additional minor adjustments were made to the size and shape of the jet profile, floc weir, and other components.

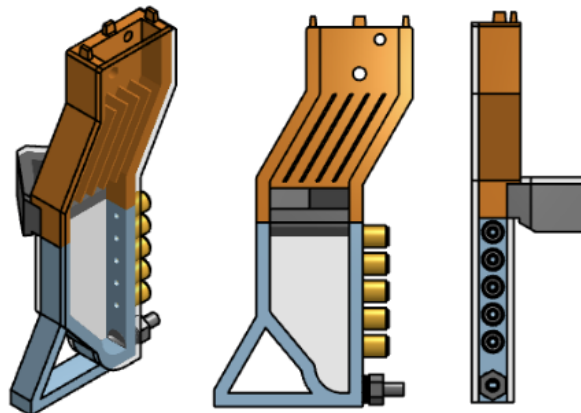


Figure 2. Schematic of revised model clarifier fabricated by the Summer 2025 team.

The Summer 2025 team used this revised model clarifier to test a procedure for measuring floc saturation inspired by Hurst et al. (2014b). First, a floc filter was formed in the clarifier by running white kaolin clay and poly-aluminum chloride (PACl) coagulant through a tube flocculator to make uncolored flocs. Then, colored clay primary particles were added to the clarifier directly. The expectation was that these colored particles would be captured by the flocs within the floc filter, leading to a color change in the more saturated regions of the clarifier. A diagram of the experimental apparatus used is pictured in Figure 3. Following the addition of colored clay, pictures of the floc filter were taken for further analysis.

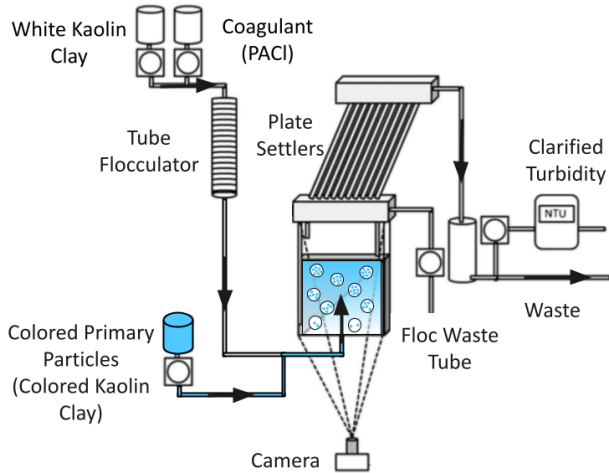


Figure 3. A diagram of the proposed experimental apparatus for detecting variations in floc saturation within the floc filter. Adapted from Hurst et al., 2014a.

Each floc filter image was processed in ImageJ by separating red, green, and blue channels, cropping to the filter region, and calculating average pixel brightness by row to assess how brightness changed with height. Unfortunately, it appeared that variations in lighting intensity influenced results far more than coloration differences, and no direct connection could be drawn between floc saturation and color intensity. Thus, the effectiveness of the floc filter imaging method remained unclear. This prompted the adoption of the new experimental procedure being used this semester.

Literature Review

Floc Bond Strength

This semester we conducted a literature review through the review paper of Jarvis et al. (2005), which provides a foundational framework for understanding floc formation and breakage dynamics in water treatment systems. According to Jarvis et al., floc growth reaches equilibrium when aggregation and breakage forces balance, mathematically expressed as the collision rate multiplied by efficiency minus the breakage rate. Two key mechanisms of breakage are highlighted: surface erosion, where tangential shear stress removes particles from floc surfaces, and large scale fragmentation, where tensile stress splits flocs into similar sized pieces. The review categorizes measurement techniques into macroscopic and microscopic approaches. Macroscopic methods include the floc strength factor, which quantifies the ratio of floc size before and after shear exposure, and shear based models that link floc size to applied velocity gradients. Microscopic methods, on the other hand, involve micromechanical tests that measure tensile rupture forces and micromanipulation techniques that compress flocs, though the latter has limited operational relevance.

A consistent theme across studies is that smaller flocs are inherently stronger than larger ones. This is attributed to increased compaction, higher bond density per unit volume, and the selective removal of weaker bonds during breakage, which leaves behind stronger remnants. Coagulation chemistry also plays a critical role in floc stability. Optimum coagulant dosing produces maximum floc strength, but this does not increase linearly with dose; instead, strength peaks and then declines at intermediate concentrations before recovering at higher levels, as described by Francois (1987) and Bache et al. (1999). Furthermore, bridging mechanisms such as sweep flocculation tend to yield stronger flocs than charge neutralization, while polymer additions show mixed outcomes, enhancing strength in chemical flocs but reducing stability in biological systems.

Recent comparisons, such as those by Yukselen and Gregory (2004), reveal that hydrolyzing coagulants like alum and polyaluminium chloride produce weaker flocs than cationic polyelectrolytes, challenging the assumption that metal coagulants are always the most effective. Jarvis et al. further argue that perfect charge neutralization may actually weaken flocs by causing particles to stick at first contact rather than reorganize into stronger structures. Instead, slight under or overdosing may enhance resilience by maintaining controlled repulsion, which allows for structural optimization. This perspective suggests that current coagulation practices may be optimized for aggregation efficiency rather than long term floc strength, offering an explanation for why many treatment plants achieve good initial removal yet still encounter floc breakage problems. More recent studies, particularly those examining interactions between polyaluminium chloride and humic acids, extend this discussion but remain underexplored, pointing to an important direction for future research.

Flocculation Modeling

Although our research this semester did not focus on flocculation, we performed a comparative review of the AguaClara flocculation model described by Pennock et al. (2018) and the model proposed by Saffman and Turner (1956). While Saffman and Turner's model was originally applied to collisions between water droplets in clouds, the model can be applied analogously to collisions between particles during flocculation. The primary difference between the two models is that the Saffman and Turner model suggests a second order rate equation for primary particle removal, while the AguaClara model suggests a 5/3 rate order. The goal of our review was to identify the differing assumptions which lead to this discrepancy.

Saffman and Turner assume droplets have no relative velocity caused by inertia or gravity, and thus move exactly with the fluid (1956). This is justified by noting that cloud droplets are extremely small, so their relaxation time (time needed for a particle to adjust to its surrounding fluid motion) is extremely short. Under this assumption the droplets will essentially behave as fluid tracers, meaning they do not slip, settle, or have inertial lag. As a result, all collisions come from purely the motion of the fluid and not from droplets overtaking each other or settling at different speeds.

It's important to note that this assumption is only reasonable for very small particles. Otherwise, fluid deformation around particles results in curvilinear strain fields, and the inertia of the particles causes them to have their own motion independent of the fluid flow. Real flocs have bigger size, inertia, and porosity than water droplets in clouds, which violates the assumptions of the derivation and may explain the different rate-law scaling.

The second assumption Saffman and Turner make is that the turbulent flow is isotropic. Their model assumes that at small enough scales, turbulence behaves the same in all directions. This is a standard Kolmogorov assumption and allows Saffman and Turner to express the collision problem entirely in terms of the energy dissipation rate ϵ and the viscosity ν , which significantly simplifies their calculations. While the AguaClara model does not directly make this assumption, its derivation is largely agnostic to the direction of the motion of particles, which leads to similar results.

The AguaClara model does make a similar assumption that the average velocity gradient does not vary significantly over space. It uses the Camp-Stein velocity gradient, or the root-mean-squared velocity gradient, as the velocity gradient throughout the flocculator (Weber-Shirk, n.d.). Due to the lack of variation, the average relative velocity between two colliding particles can be expressed as a function of the separation distance between the particles. This assumption is partially validated by the intentional design of AguaClara flocculators to minimize the variation in velocity gradient (Weber-Shirk, n.d.). The Saffman and Turner model makes the slightly more nuanced assumption that velocity gradient is normally distributed. However, assuming an entirely uniform velocity gradient only changes the final collision rate by a constant factor.

The third assumption made is that droplet size is much smaller than the Kolmogorov length scale, which is the size of the smallest eddies in a turbulent flow. Below this scale, the flow behaves like a locally linear shear field instead of a swirl. Saffman and Turner argue that because the droplets are much smaller than this scale, the velocity field which they experience is essentially linear. This has two important consequences, the first being that the flow around each droplet can be approximated as a uniform strain field because the relative motion between two droplets near each other depends only on the local velocity gradient. The second consequence is that instead of needing the full turbulent velocity field, Saffman and Turner only need the statistical properties of the small-scale velocity gradients, which are already known from Kolmogorov theory.

However, the AguaClara model argues that the size of the droplets being smaller than the Kolmogorov length scale is insufficient to claim that they experience a linear velocity field. Rather, Pennock et al. argue that the relative velocity between two particles should scale with the particle separation distance. Hence, the particle separation distance must be smaller than the Kolmogorov length scale for this simplification to be valid. While the AguaClara model does ultimately assume that the particle separation distance is smaller than the Kolmogorov length scale, this is still an important distinction between the two models.

The fourth assumption made by Saffman and Turner is that particles do not significantly distort the flow around them. They assume that the paths traveled by particles are more or less the same as the paths they would travel in if no other particles were present in the fluid. This is validated through experimental data for similarly sized particles. Saffman and Turner primarily focus on equal-sized droplets. This was particularly important because earlier models had predicted zero collision rate between equal particles. The AguaClara model takes this assumption one step further. Based on the results of Casson and Lawler, it assumes that collisions *only* occur between similarly sized particles (1990). This is a result of boundary layer effects which prevent collisions between particles of different sizes.

The fifth assumption is that droplets are uniformly mixed throughout the fluid. This means that averaging over turbulence statistics also correctly averages over droplet positions, and there is no need to account for clustering or preferential concentration. The AguaClara model also makes this assumption implicitly.

The Saffman and Turner model culminates in a collision kernel that scales with $(r_1 + r_2)^3$. Saffman and Turner show that the rate at which two droplets collide depends on the volume of the ‘collision sphere’ (radius = $r_1 + r_2$) and the average radial velocity induced by the local strain. Collision rate also depends only on small-scale turbulence ε and v , the energy dissipation rate and kinematic viscosity. This happens because under the assumptions of isotropy and small particle size, the local velocity gradients follow Kolmogorov scaling. The final collision kernel is $K \propto (r_1 + r_2)^3 \left(\frac{\varepsilon}{v}\right)^{1/2}$. Larger droplets experience proportionally faster convergence, which gives them a much higher collision rate.

Overall, this review provided a number of avenues to explore in future research on how the assumptions of the AguaClara Flocculation model compare to other models. While no individual assumption stood out as the key factor which could explain the difference between the two models, the differences we identified could provide opportunities to improve the AguaClara model in the future.

Red-40 Dye Selection

The dye Red-40 was evaluated for its potential usage in flocculation/clarification experiments. Red-40 is an anionic azo dye with sulfonate groups that impart a negative charge in aqueous solutions; it has chemical formula C₁₈H₁₄N₂Na₂O₈S₂ and molecular weight 496.4 g-mol-1.

Existing literature focused on adsorption of Red-40 onto chitosan. According to Kumar et al. (2000), chitosan is a cationic polysaccharide that is made from chitin deacetylation; chitin is found in insect exoskeletons, crustaceans shells, and fungal cell walls. Pinto et al. (2009) demonstrated that the protonated amino group in chitosan yields a positive charge, facilitating strong electrostatic interactions with the negatively charged sulfonate groups on Red-40 and leading to strong adsorption between chitosan and Red-40.

Pinto et al. (2011) demonstrated the Red-40 adsorption onto chitosan follows pseudo-second-order and Elovich kinetic models, suggesting that the adsorption occurs through chemical interactions in addition to physical interactions. Infrared spectroscopy results showed evidence of the electrostatic interaction between the amine group of chitosan and the sulfonated group of Red-40. Furthermore, thermodynamic data from Pinto et al. (2009) indicate the adsorption of Red-40 on chitosan is an exothermically-controlled process. These findings indicate that Red-40 adsorption onto chitosan is favorable.

PACl Coagulant and chitosan shared key characteristics that showed promise for Red-40 adsorption onto coagulant. Both chitosan and coagulant have a net positive surface charge under acidic to near-neutral pH, favoring adsorption of anionic dyes such as Red-40. The aluminum hydroxide complexes in coagulant can act in a manner similar to protonated amine groups in chitosan, interacting with Red-40's sulfonated group. Thus, the use of Red-40 as a dye for the floc filter showed promise.

Methylene Blue Dye Selection

The dye methylene blue was also evaluated for its potential usage in flocculation and clarification experiments. Methylene blue is a cationic dye with molecular formula C₁₆H₁₈N₃SCl and molecular weight 319.85 g-mol⁻¹.

Because methylene blue is cationic, and kaolinite clay has a negative charge, electrostatic attraction allows for the adsorption of methylene blue onto kaolinite clay. Since PACl coagulant has a positive charge, methylene blue showed promise in interacting with kaolin without much interference from the coagulant. Ghosh and Bhattacharyya (2002) found that raw kaolin showed a “considerable adsorption”, and NaOH-treated pure kaolin could adsorb almost 100% methylene blue from a 12-ppm solution. Adsorption showed a minimum at a pH of around four, with adsorption increasing as pH increases. Data from Ghosh and Bhattacharyya (2002) fit both Langmuir and Freundlich isotherms, with a Freundlich exponent *n* between 0.047 and 0.151 indicating favorable adsorption. Raw kaolin clay fits inside this range, indicating favorable absorption of methylene blue onto raw kaolin clay.

Furthermore, Ghosh and Bhattacharyya (2002) observed that the adsorption of methylene blue has a negative standard Gibbs energy change, and is endothermic with positive entropy, showing that adsorption is spontaneous and thermodynamically favorable. Due to these factors, methylene blue was selected as a dye for testing.

Clarification Modeling

Vitasovic (1986) and Takacs et al. (1991) developed a 1D model of clarification based on solids flux theory to predict the sludge blanket settling velocity. The Takacs model unified the description of both discrete and hindered settling into a single equation. However, Gernaey et al. (2001) highlighted the difficulty of fitting this model, limiting its utility in practical applications. Head et al. (1997) modeled floc blanket clarification by examining how influent concentration and floc wastage flow rate influence the height and concentration of the floc blanket. However,

the model is limited in its ability to describe how particle size distribution post-flocculation and coagulant dosage impact clarification performance.

Sarmiento (2021) addressed this gap by applying the Pennock et al. (2018) flocculation model which accounts for coagulant dosage and distinguishes between the settleable and non-settleable particles formed during flocculation. Sarmiento (2021) assumes that all settleable particles generated during flocculation are removed during clarification. In contrast to model predictions, experimental results indicate that clarification performance decreases over time, possibly due to effects of floc saturation. Pennock et al. (2023) modified the Pennock et al. (2018) flocculation model to describe how the conversion from non-settleable to settleable particles depends on clarifier design. Nonetheless, their work did not incorporate floc sweeping and floc saturation, which are of significance in floc filter-based clarifiers. In the summer of 2024, our team built on these models to account for floc sweeping and floc saturation. Despite these enhancements, discrepancies between experimental and theoretical parameter values exist, indicating the need to reevaluate the assumptions of the model. The major assumptions are that flocs in the floc filter are at their steady-state saturation level and the floc filter is well-mixed. Therefore experimentation is needed to investigate the spatial and temporal dynamics of the floc filter. This semester, the subteam will look into whether floc movement probabilities between positions remain constant across time steps ie. testing if flocs move independently rather than collectively in discrete layers.

Methods

Experimental Apparatus

For our experiments, we used a tube flocculator paired with the low hydraulic residence time model clarifier developed by the Summer 2025 team. The tube flocculator had a radius of curvature of 42 mm and an inner diameter of 4.381 mm. Based on calculations described by Tse et al. (2011), at a flow rate of 1.2 mL/s, this gave a velocity gradient of $G = 145 \text{ Hz}$. This flow rate also gave a hydraulic residence time of $\theta = 304 \text{ seconds}$.

The parameters of the clarifier were chosen to mimic the characteristics of an actual AguaClara clarifier. The cross-sectional area of the clarifier was designed to be 1200 mm^2 in order to achieve an upflow velocity of 1 mm/s given a flow rate of 1.2 mL/s since this is the upflow velocity used in AguaClara plants (Weber-Shirk, n.d.). The average initial velocity at the jet was 17 mm/s based on the cross-sectional area of the jet inlet, which was 71 mm^2 . This larger initial velocity ensured the jet would have sufficient momentum to keep the floc filter suspended.

For the plate settlers, a spacing of 1 cm between plates was chosen to avoid floc rollup. Using the equation found in the AguaClara textbook (Weber-Shirk, n.d.), we calculated the necessary plate settler length to be 14.67 cm to ensure the AguaClara standard capture velocity of 0.12 mm/s. However, due to limitations in print size, we chose to reduce the length to 7.33 cm, resulting in a capture velocity of 0.21 mm/s. A plate width of 2.0 mm was chosen to balance the integrity of the print with having the thinnest plates possible to reduce the increase in upflow velocity through the plate settlers. The plates were placed at a 60° angle based on AguaClara

clarifier specifications (Weber-Shirk, n.d.). The area above the plate settlers was left open to the air to prevent air bubbles from being trapped in a closed system.

During operation, coagulant and a turbidity source (typically white kaolin clay) were first added to the influent of the tube flocculator. After exiting the flocculator, the newly formed flocs were directed into the clarifier. The jet reverse maintained these flocs in suspension in order to form a floc filter within the clarifier. Excess flocs were removed via a floc hopper, which drained flocs from the floc filter once they reached a height of 124 mm above the diffuser.

Apparatus Revisions

Towards the end of our experiments, the model clarifier began leaking significantly, necessitating the creation of a new clarifier. Figures 4(a), 4(b), and 5 show the changes made to the design. To reduce the potential of leakage, the sampling ports along the side, depicted in Figure 4(c), were removed. Additionally, to improve the adhesion between the front acrylic plate and the clarifier body, a lip was added, extending from the clarifier body to surround the edge of the acrylic plate. Finally, the floc hopper was extended such that the floor sloped downward. This encourages sludge that has entered the floc hopper to slide down towards the waste port and prevents excess flocs from building up in the floc filter.

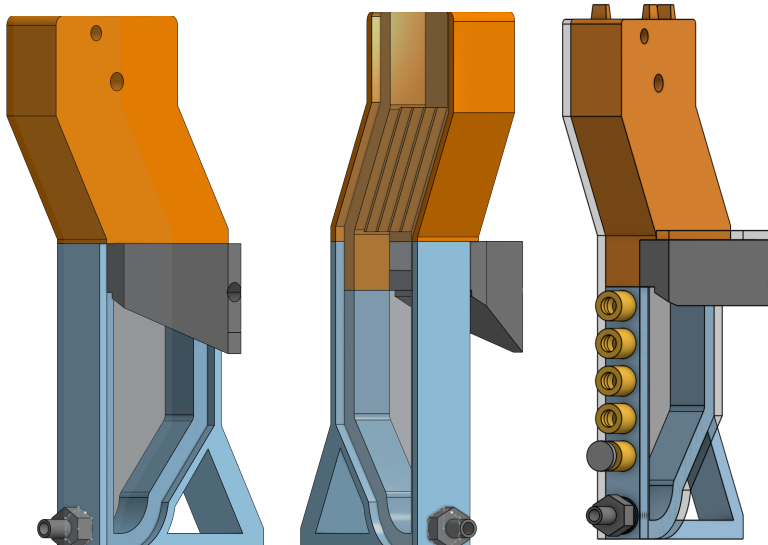


Figure 4(a), (b), (c). Downward sloping floc hopper and sample ports removed in revised clarifier (left), lip added to clarifier body surrounding acrylic plate (middle), and old clarifier with sampling ports, flat-bottomed floc hopper, and no lip (right).

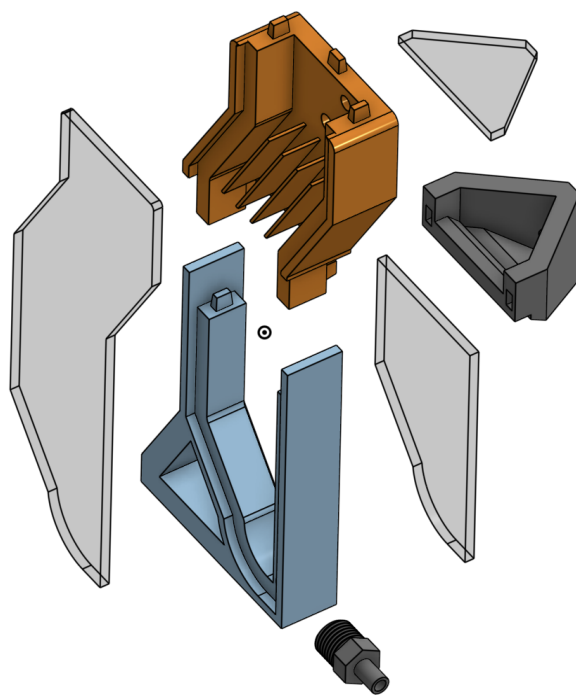


Figure 5. Exploded view of new clarifier design.

Experimental Design

Our proposed method for tracking the movement of flocs within the floc filter is as follows. First, a colorless floc filter will be formed from white kaolin clay and poly-aluminum chloride (PACl) coagulant. Next, a small number of colored flocs will be formed by combining Red-40, white kaolin clay, and PACl. The white kaolin clay will still make up the majority of the contents of the flocs so that their properties are comparable to the uncolored flocs. These colored flocs will then be inserted into the clarifier, allowing us to track the movement of these tracer flocs within the floc filter. Figure 6 shows a process flow diagram of this full process. From this, we can determine if the motion of flocs within the floc filter is independent of their current location or if the flocs tend to move in discrete sections. If the movement is random and the colored flocs quickly become uniformly distributed within the floc filter, then it follows that floc saturation will also be uniformly distributed within the clarifier.

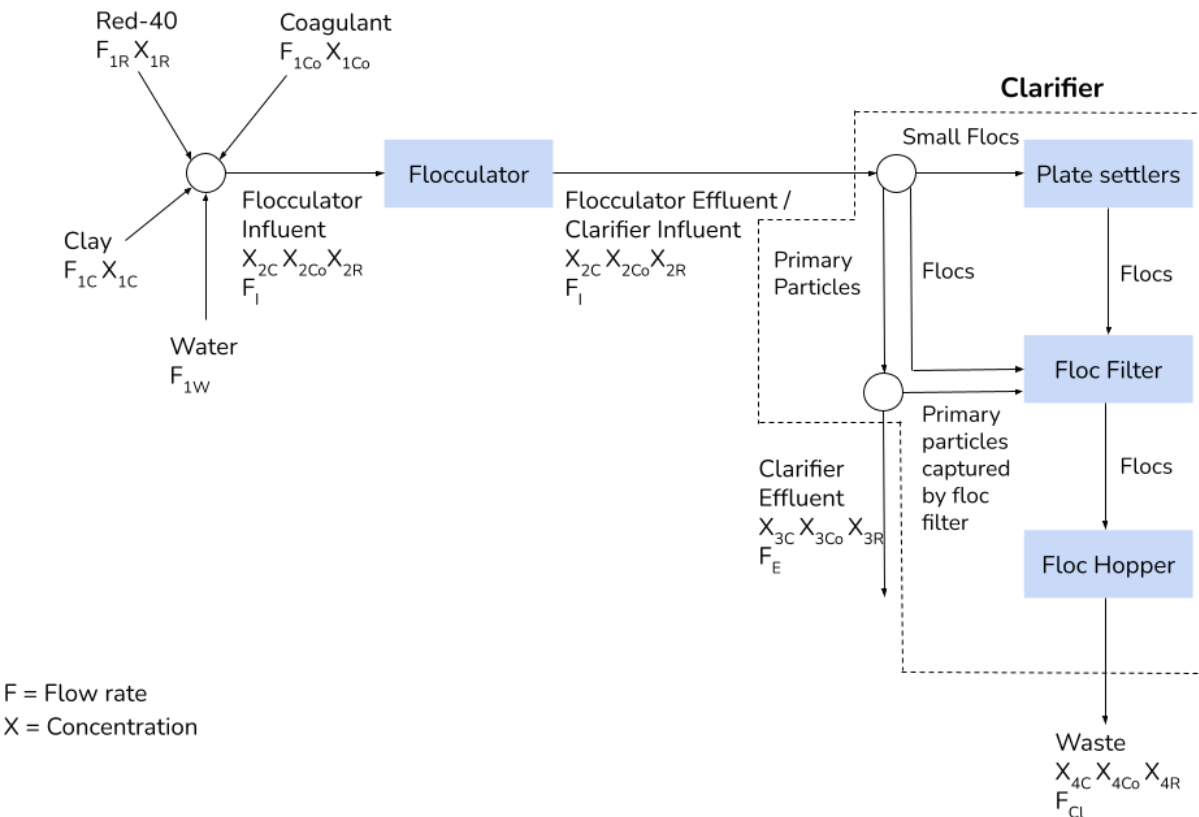


Figure 6. Process flow diagram illustrating movement of clay, coagulant, and Red-40 through the experimental setup.

In order to ensure that this procedure would work, we first had to verify that we could make colored flocs using Red-40. We tested this in two phases. First, we attempted to form colored flocs using only Red-40 and PACl . A solution of 40 mg/L of Red-40 and 10 mg/L of PACl was added to the flocculator over the course of 80 minutes, providing ample time for floc filter formation. Due to an oversight when initializing the ProCoDA method file, a flow rate of 1.3 mL/s was used rather than the typical 1.2 mL/s. After 20 minutes had elapsed, the concentration of PACl was increased to 20 mg/L to promote larger floc formation.

In the second phase, we attempted to form flocs containing both kaolin clay and Red-40. Over the course of 15 minutes, a solution of 46 mg/L of white kaolin clay, 4 mg/L of Red-40, and 20 mg/L of PACl was added to the flocculator. After testing for the formation of colored flocs, we continued building the floc filter using a solution of 50 mg/L of white kaolin clay and 20 mg/L of PACl in order to test if the colored flocs could be distinguished from uncolored flocs.

After these initial tests, we tried implementing our procedure for tracking the movement of flocs in the floc filter. A solution of 50 mg/L of white kaolin clay and 20 mg/L of PACl was added to the flocculator over the course of 50 minutes in order to form an uncolored floc filter.

Afterwards, a solution of 46 mg/L of white kaolin clay, 4 mg/L of Red-40, and 20 mg/L of PACl was added for 10 minutes in order to introduce a small number of colored flocs. Finally, the influent solution was returned to the original 50 mg/L of white kaolin clay and 20 mg/L of PACl in order to monitor the movement of the colored flocs over an additional 20 minutes.

Jar Tests

In addition to our primary tracer floc experiments, we also conducted jar tests to determine the ideal dosages of PACl, Red-40, and clay. Our goal was to determine a dosage of Red-40 that would make the tracer flocs clearly distinguishable without leaving excess Red-40 in solution that could adsorb onto the non-tracer flocs. We experimented both with and without clay in the tracer flocs as previous visualization experiments using only dye in flocs without clay had shown greater success (Weber-Shirk, n.d.). Initial tests did not include a rapid mix phase, but a rapid mix phase was later introduced to ensure efficient mixing. For each experiment, the total volume of solution prepared was 750 mL. The flocculation phase for all tests was conducted at a speed of 30 RPM, and each test was allowed to run for around 50 minutes to ensure the fullest extent of flocculation. The full set of experiments is shown in Table 1.

Clay Concentration (mg/L)	PACl Concentration (mg/L)	Red-40 Concentration (mg/L)	Rapid Mix?
10	2	0.5	No
10	2	1	No
10	2	2	No
10	4	2	No
10	6	2	No
0	20	40	No
0	2	10	Yes
0	2	5	Yes
0	2	2.5	Yes
0	4	5	Yes

Table 1. Jar Tests Using Red-40.

We also conducted two jar tests using methylene blue as a possible alternative to Red-40. Because methylene blue is cationic, it must adsorb onto the negatively charged clay instead of the positively charged PACl. For this reason, we mixed the clay and methylene blue solutions

together before introducing the PACl . This provided the methylene blue ample time to adsorb onto the clay before flocculation. We used a fixed ratio of 13 mg of methylene blue per 1000 mg based on the work done by Ghosh and Bhattacharyya (2002). These tests used the same mixing speed and overall setup as the previous tests with Red-40. The solution concentrations are shown in Table 2.

Clay Concentration (mg/L)	PACl Concentration (mg/L)	Methylene Blue Concentration (mg/L)	Rapid Mix?
10	4	0.13	Yes
10	10	0.13	Yes

Table 2. Jar Tests Using Methylene Blue.

Results

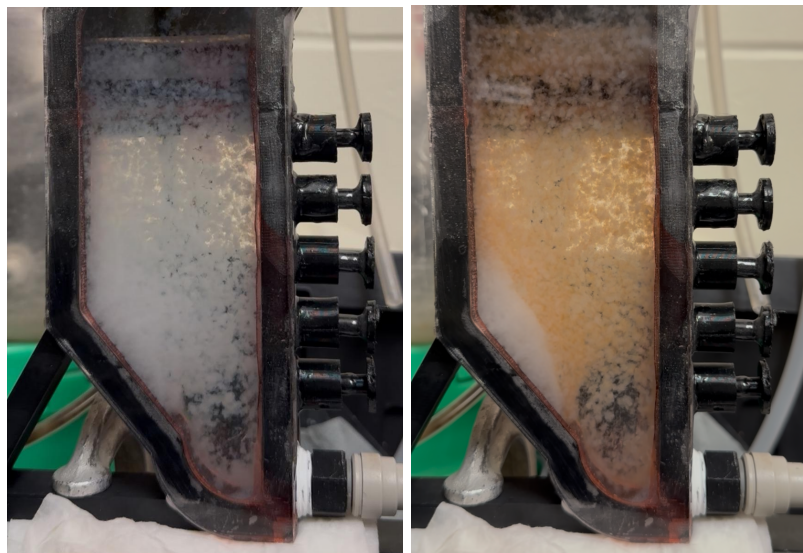
The initial experiment for forming flocs from Red-40 and PACl showed promising results. The Red-40 successfully formed large, healthy flocs to populate the floc filter, as shown in Figure 7. Residual dissolved Red-40 in the clarifier which had not been incorporated into flocs caused the water to be dyed a deep red. Although this made it harder to see the colored flocs, this behavior was expected due to the extremely high concentration of Red-40 being used.



Figure 7. Floc filter formed from Red-40 and PACl .

The flocs formed from Red-40 combined with white kaolin clay were also promising. While the coloration was lighter due to the smaller concentration of Red-40, the flocs were still distinctly red. As a side effect of the lower Red-40 concentration, there was also less residual Red-40 to dye the water, meaning the flocs did not blend in as much with the surrounding water. However, after ceasing the addition of Red-40, the flocs entering the floc filter continued to be red. Even after 25 minutes of adding white kaolin clay flocs without any additional Red-40, the entire floc filter remained the same color, with no discernible differentiation between the colored and uncolored flocs.

The results of the last experiment were similar. We hypothesized that the continued red coloration could have been coming from residual Red-40 that was stuck to the walls of the flocculator, so before starting the experiment, we cleaned the flocculator using distilled vinegar in order to neutralize any PACl which was allowing the Red-40 to adhere to the walls. This seemed to work as the initial uncolored floc filter formed successfully without any red coloration, as seen in Figure 8(a). However, once the Red-40 was added, the coloration quickly spread throughout the entire floc filter as shown in Figure 8(b), with the exception of a small corner of the diffuser where the flocs did not appear to be suspended properly, preventing dye from reaching them.



Figures 8(a), (b). Floc filter (a) before and (b) after addition of Red-40.

The Red-40 jar tests did not provide any possible solutions for this problem. In all Red-40 trials, visible flocs formed, showing that coagulation and aggregation were occurring as expected. We found that a minimum of 2 mg/L of Red-40 was necessary to produce visually distinguishable red flocs. However, at this concentration, the water in the jar remained noticeably red as seen in Figure 9, suggesting that most of the dye was not fully removed from solution. This remained true regardless of the coagulant dose. These results suggest that Red-40 attached

loosely to the flocs but did not bond strongly enough to be fully captured or removed, or that the amount of excess Red-40 that remained in solution was sufficient to dye non-tracer flocs.



Figure 9. Jar test containing 10 mg/L of clay, 2 mg/L of PACl , and 2 mg/L of Red-40. After flocculation, the solution is still noticeably red.

The methylene blue trials produced a different outcome. When methylene blue was introduced through dyed clay, the resulting flocs were richly colored and compact, forming rapidly and settling with clear definition. Unlike with the Red-40, Figure 10 shows that the color of the methylene blue was largely removed from the solution. Although the water retained a faint tint, most of the dye appeared to be captured within the aggregates themselves, indicating stronger adsorption and a more stable association between the dye and the floc surfaces. The distinct coloration of the settled solids made it easy to visually confirm floc development.



Figure 10(a), (b). Jar tests with 10 mg/L of clay, 0.13 mg/L of methylene blue, and (a) 10 mg/L of PACl or (b) 4 mg/L of PACl .

Discussion

Based on the manner in which the coloration spread through the floc filter after the addition of Red-40, it is likely that residual dissolved Red-40 that has not been flocculated is spreading throughout the clarifier and quickly adsorbing onto flocs, leading to the sudden color change observed throughout the floc filter. Unfortunately, the jar tests indicate that it is infeasible to remove all Red-40 from solution through flocculation. It should be noted that the coagulant used for the jar tests was outdated (prepared over 1 year ago), which may have contributed to the poor removal. Regardless, the results indicate that Red-40 may not be a viable choice as a tracer dye within the clarifier.

On the other hand, methylene blue shows significant potential for use as a tracer dye. Its stable adsorption onto clay prevents the dye from diffusing back out of the tracer flocs and onto non-tracer flocs. Furthermore, unlike with Red-40, the amount of methylene blue can be adjusted to ensure that almost all the methylene blue is removed from solution and adsorbed onto flocs. This leaves very little methylene blue in solution to adsorb onto non-tracer flocs and makes it easier to visually distinguish between tracer and non-tracer flocs in the clarifier.

Future Work

Following the successful formation of methylene blue-dyed flocs that were easy to visualize and did not leach color, we will discontinue using Red-40. Instead, methylene blue dye will be used to create blue tracer flocs. We will track the movement of blue tracer flocs through the white floc filter and qualitatively analyze its spatial distribution. Eventually, we aim to use image processing and analysis to quantitatively describe how tracer flocs move in the floc filter.

In addition to switching from Red-40 dye to methylene blue dye, we will resin print and assemble the revised clarifier. The new clarifier will be utilized in future experiments and improve experimental efficiency and the quality of results.

Appendix

Section I: Mass Balance Calculations for Experimentation

Total influent flow rate (mL/s)	1.2
Effluent flow rate (mL/s)	1.2
Clay/coagulant/Red-40 influent flow rate (mL/s)	x
Clay/coagulant/Red-40 influent concentration (M)	c
Clay/coagulant/Red-40 stock concentration (M)	s

Clay/coagulant/Red-40 pump volume per revolution (mL/rev)	n
Clay/coagulant/Red-40 pump speed (rev/s)	v
Water flow rate (mL/s)	w
Waste flow rate (mL/s)	a
Effluent with wasting flow rate (mL/s)	e

The equations below were used to determine the flow rates and pump speeds during the experiment.

$$x = \frac{1.2 c}{s}$$

$$v = \frac{60 x}{n}$$

$$w = 1.2 - x_{clay} - x_{coag} - x_{red}$$

$$e = 1.2 - a$$

Manual

Experiment SOP

Creating stock solutions

Stock solutions were created and stored in 1 L bottles. In the model-clarifier setup, magnetic stir bars were placed in each solution to ensure particles remained suspended and evenly distributed throughout the solution.

Pumps and Machines

Insert the tubes connected to pumps into the corresponding bottles of stock solution. The tubes can be inserted into hollow acrylic rods to prevent them from falling out of the bottles. Turn on the water pipe by turning the water lever in Hollister B60 until it is at a 45° angle. Then, turn on the lab computer, turbidimeters, and all pumps. Using the “Just Water” state, run water through the system for ten minutes to flush out residual chemicals.

Cleanup

When experiments have concluded, turn off pumps, turbidimeters, and the lab computer. Empty the clarifier, and seal stock solution bottles. Unused coagulant stock solution should be disposed of as coagulant quickly loses effectiveness once diluted.

Troubleshooting

If there are air bubbles entering the clarifier, poke a needle into the tube or insert a smaller tube to release air. Furthermore, raising the lower end of the tube leverages pressure differences to purge air bubbles. If pumps or turbidimeters are not connecting to the computer, turn them off and restart ProCoDA; ensure that the ID's and settings on ProCoDA are correct. If turbidimeter readings are inaccurate, check and clean the turbidimeter for residual particles and/or recalibrate the device.

Mini-Clarifier Fabrication

The main body of the mini-clarifier was printed from HDPE in three separate parts at Cornell's Rapid Prototyping Lab: the diffuser, the plate settlers, and the floc hopper. These parts were assembled and glued together using epoxy. The acrylic plates used for the front and back of the clarifier and the top of the floc hopper were laser cut and also attached using epoxy. The influent jet nozzle was not epoxied into place; rather, it was threaded into the main body using teflon tape to allow for future modifications. Threaded adapters were used to attach tubing to different points on the mini-clarifier including the influent nozzle, overflow tube, and waste tube.

References

- Bache, D. H., Rasool, E., Moffat, D., & McGilligan, F. J. (1999). On the strength and character of Alumino-Humic Flocs. *Water Science and Technology*, 40(9).
- [https://doi.org/10.1016/s0273-1223\(99\)00643-5](https://doi.org/10.1016/s0273-1223(99)00643-5)
- Casson, L. W., & Lawler, D. F. (1990). Flocculation in turbulent flow: Measurement and modeling of particle size distributions. *Journal AWWA*, 82(8), 54–68.
- <https://doi.org/10.1002/j.1551-8833.1990.tb07010.x>
- François, R. J. (1987). Strength of aluminium hydroxide flocs. *Water Research*, 21(9), 1023–1030. [https://doi.org/10.1016/0043-1354\(87\)90023-6](https://doi.org/10.1016/0043-1354(87)90023-6)
- Gernaey, K., Vanrolleghem, P. A., & Lessard, P. (2001). Modeling of a reactive primary clarifier. *Water Science & Technology*, 43(7), 73–81. <https://doi.org/10.2166/wst.2001.0393>
- Ghosh, D., & Bhattacharyya, K. G. (2002). Adsorption of methylene blue on kaolinite. *Applied Clay Science*, 20 (6), 295–300. [https://doi.org/10.1016/S0169-1317\(01\)00081-3](https://doi.org/10.1016/S0169-1317(01)00081-3)
- Head, R., Hart, J., & Graham, N. (1997). Simulating the effect of blanket characteristics on the floc blanket clarification process. *Water Science & Technology*, 36(4).
- [https://doi.org/10.1016/s0273-1223\(97\)00422-8](https://doi.org/10.1016/s0273-1223(97)00422-8)
- Hurst, M., Weber-Shirk, M., Charles, P., & Lion, L. W. (2014a). Apparatus for observation and analysis of Floc Blanket Formation and performance. *Journal of Environmental Engineering*, 140(1), 11–20. [https://doi.org/10.1061/\(asce\)ee.1943-7870.0000773](https://doi.org/10.1061/(asce)ee.1943-7870.0000773)

- Hurst, M., Weber-Shirk, M., & Lion, L. W. (2014b). Image analysis of floc blanket dynamics: Investigation of floc blanket thickening, growth, and steady state. *Journal of Environmental Engineering*, 140(4). [https://doi.org/10.1061/\(asce\)ee.1943-7870.0000817](https://doi.org/10.1061/(asce)ee.1943-7870.0000817)
- Jarvis, P., Jefferson, B., Gregory, J., & Parsons, S. A. (2005). A review of floc strength and breakage. *Water Research*, 39(14), 3121–3137. <https://doi.org/10.1016/j.watres.2005.05.022>
- Kumar, M. N. V. R. (2000). A review of chitin and chitosan applications. *Reactive and Functional Polymers*, 46(1), 1–27. [https://doi.org/10.1016/S1381-5148\(00\)00038-9\[1\]](https://doi.org/10.1016/S1381-5148(00)00038-9[1])
- Pennock, W. H., Weber-Shirk, M. L., & Lion, L. W. (2018). A hydrodynamic and surface coverage model capable of predicting settled effluent turbidity subsequent to hydraulic flocculation. *Environmental Engineering Science*, 35(12), 1273–1285. <https://doi.org/10.1089/ees.2017.0332>
- Pennock, W. H., Lion, L. W., & Weber-Shirk, M. L. (2023). Simple model for coupled hydraulic flocculation-sedimentation performance. *Journal of Environmental Engineering*, 149(12). <https://doi.org/10.1061/joeedu.eeeng-7384>
- Piccin, J. S., Dotto, G. L., Vieira, M. L. G., & Pinto, L. A. A. (2009). Adsorption of FD&C Red No. 40 by chitosan: Isotherms analysis. *Chemical Engineering Journal*, 150(2–3), 366–373. <https://doi.org/10.1016/j.jfoodeng.2009.03.017>
- Piccin, J. S., Vieira, M. L. G., Dotto, G. L., & Pinto, L. A. A. (2011). Kinetics and mechanism of the food dye FD&C Red 40 adsorption onto chitosan. *Journal of Chemical & Engineering Data*, 56(10), 3759–3765. <https://doi.org/10.1021/je200388s>
- Saffman, P.G., & Turner, J. S. (1956). On the collision of drops in turbulent clouds. *Journal of Fluid Mechanics*, 1(01), 16–16. <https://doi.org/10.1017/s0022112056000020>
- Sarmiento, K. (2021). Particle Removal in Floc Blanket Clarifiers Via Internal Flow Through Porous Fractal Aggregates. *Cornell University*.
- Takács, I., Patry, G., & Nolasco, D. (1991). A dynamic model of the clarification-thickening process. *Water Research*, 25(10), 1263–1271. [https://doi.org/10.1016/0043-1354\(91\)90066-y](https://doi.org/10.1016/0043-1354(91)90066-y)
- Tse, I. C., Swetland, K., Weber-Shirk, M. L., & Lion, L. W. (2011). Method for quantitative analysis of flocculation performance. *Water Research*, 45(10), 3075–3084. <https://doi.org/10.1016/j.watres.2011.03.021>
- Vitasovic, Z. Z. (1986). An Integrated Control Strategy for the Activated Sludge Process. Rice University.

Weber-Shirk, M. (n.d.). *The Physics Of Water Treatment Design*.

<https://aguaclara.github.io/Textbook/index.html>

Yukselen, M. A., & Gregory, J. (2004). The effect of rapid mixing on the break-up and re-formation of Flocs. *Journal of Chemical Technology & Biotechnology*, 79(7), 782–788. <https://doi.org/10.1002/jctb.1056>